NeuroImage 256 (2022) 119212

Contents lists available at ScienceDirect

NeuroImage

journal homepage: www.elsevier.com/locate/neuroimage

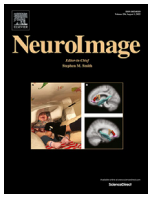

Diagnosis-informed connectivity subtyping discovers subgroups of autism with reproducible symptom profiles

Hyoungshin Choi[a,b,1], Kyoungseob Byeon[a,b,1], Bo-yong Park[b,c], Jong-eun Lee[a,b], Sofie L. Valk[d,e,f,g], Boris Bernhardt[h], Adriana Di Martino[i], Michael Milham[j,k], Seok-Jun Hong[b,j,l,*], Hyunjin Park[b,m,*]

[a] Department of Electrical and Computer Engineering, Sungkyunkwan University, Suwon, South Korea
[b] Center for Neuroscience Imaging Research, Institute for Basic Science, Suwon, South Korea
[c] Department of Data Science, Inha University, Incheon, South Korea
[d] Otto Hahn group, Cognitive neurogenetics, Max Planck Institute for Human Cognitive and Brain Sciences
[e] Institute of Neuroscience and Medicine, Research Centre Jülich, Jülich, Germany
[f] Institute of Systems Neuroscience, Medical Faculty, Heinrich Heine University Düsseldorf, Düsseldorf, Germany
[g] Max Planck Institute for Human Cognitive and Brain Sciences, Leipzig, Germany
[h] McConnell Brain Imaging Centre, Montreal Neurological Institute and Hospital, McGill University, Montreal, Quebec, Canada
[i] Autism Center, Child Mind Institute, New York, United States
[j] Center for the Developing Brain, Child Mind Institute, New York, United States
[k] Nathan S. Kline Institute for Psychiatric Research, New York, United States
[l] Department of Biomedical Engineering, Sungkyunkwan University, Suwon 16419, South Korea
[m] School of Electronic and Electrical Engineering, Sungkyunkwan University, Suwon 16419, South Korea

ARTICLE INFO

Keywords:
Autism
Reproducibility
Neurosubtypes
Gradient
Functional random forest
Supervised-unsupervised hybrid clustering

ABSTRACT

Clinical heterogeneity has been one of the main barriers to develop effective biomarkers and therapeutic strategies in autism spectrum disorder (ASD). Recognizing this challenge, much effort has been made in recent neuroimaging studies to find biologically more homogeneous subgroups (called 'neurosubtypes') in autism. However, most approaches have rarely evaluated how much the employed features in subtyping represent the core anomalies of ASD, obscuring its utility in actual clinical diagnosis. To address this, we combined two data-driven methods, '*connectome-based gradient*' and '*functional random forest*', collectively allowing to discover reproducible neurosubtypes based on resting-state functional connectivity profiles that are specific to ASD. Indeed, the former technique provides the features (as input for subtyping) that effectively summarize whole-brain connectome variations in both normal and ASD conditions, while the latter leverages a supervised random forest algorithm to inform diagnostic labels to clustering, which makes neurosubtyping driven by the features of ASD core anomalies. Applying this framework to the open-sharing Autism Brain Imaging Data Exchange repository data (discovery, $n = 103/108$ for ASD/typically developing [TD]; replication, $n = 44/42$ for ASD/TD), we found three dominant subtypes of functional gradients in ASD and three subtypes in TD. The subtypes in ASD revealed distinct connectome profiles in multiple brain areas, which are associated with different Neurosynth-derived cognitive functions previously implicated in autism studies. Moreover, these subtypes showed different symptom severity, which degree co-varies with the extent of functional gradient changes observed across the groups. The subtypes in the discovery and replication datasets showed similar symptom profiles in social interaction and communication domains, confirming a largely reproducible brain-behavior relationship. Finally, the connectome gradients in ASD subtypes present both common and distinct patterns compared to those in TD, reflecting their potential overlap and divergence in terms of developmental mechanisms involved in the manifestation of large-scale functional networks. Our study demonstrated a potential of the diagnosis-informed subtyping approach in developing a clinically useful brain-based classification system for future ASD research.

* Corresponding authors.
E-mail addresses: hongseokjun@skku.edu (S.-J. Hong), hyunjinp@skku.edu (H. Park).
[1] These authors contributed equally to this work.

https://doi.org/10.1016/j.neuroimage.2022.119212.
Received 10 December 2021; Received in revised form 28 March 2022; Accepted 13 April 2022
Available online 14 April 2022.
1053-8119/© 2022 The Authors. Published by Elsevier Inc. This is an open access article under the CC BY-NC-ND license (http://creativecommons.org/licenses/by-nc-nd/4.0/)

1. Introduction

Autism spectrum disorder (ASD) is a pervasive developmental condition characterized by substantial heterogeneity across multiple symptoms such as impaired social cognition and altered sensory sensitivities (GUZE, 1995). While this heterogeneity is likely derived from the multiple underlying etiologies (Ronald et al., 2006; Masi et al., 2017), overarching pathogenic mechanisms remain poorly understood, mainly due to a lack of system-level evidence linking the molecular bases and behavioral manifestation (Kozak and Cuthbert, 2016). To fill this gap, recent neuroimaging studies based on fully data-driven clustering have sought to decompose ASD individuals showing complex brain-wide anomalies into more homogeneous subgroups, so-called *neurosubtypes* (Hong et al., 2018; S.J. Hong et al., 2020; Feczko et al., 2019; Wolfers et al., 2019). Indeed, regardless of imaging modality and method, these studies converged to indicate 2–4 ASD subtypes (Hong et al., 2018; S.J. Hong et al., 2020), each showing distinct cortical morphology (Hong et al., 2018; Chen et al., 2019) or functional connectivity (FC) reconfiguration (Easson et al., 2019; Tang et al., 2020), the patterns associated with different levels of behavioral symptoms.

So far, ASD subtyping has been less established in actual diagnosis. It is partly due to suboptimal subtyping approaches, as previous studies have mainly attempted to partition ASD individuals without considering how to tie the subtyping with clinical variables of interest at the level of a clustering step (Feczko et al., 2019). In other words, current approaches usually do not evaluate how much the employed neuroimaging features (*e.g.,* FC or cortical thickness) reflect the core characteristics of ASD when performing clustering; thus, even if the study discovers seemingly distinct subtypes, their clinical relevance may not be immediately obvious. Another issue limiting the current subtyping effort is that the clustering has been so far conducted mainly within the ASD population. Although simpler and parsimonious, this ASD-focused approach tends to ignore the fact that their brain-level variability often overlaps with that of other developmental conditions as well as even healthy individuals (Kanai and Rees, 2011; Kernbach et al., 2018), which significantly hampers to reveal a complete picture of ASD-specific neurobiology. This perspective (treating ASD as an independent pathological entity) may preclude the understanding of a full picture of ASD neurobiology. Recognizing all these issues, a recent study proposed a novel method called '*functional random forest*', a hybrid supervised (*i.e.,* random forest (Breiman, 2001) for diagnostic label prediction) and unsupervised (*i.e.,* Infomap-based clustering (Rosvall and Bergstrom, 2008)) algorithm in order to find ASD and TD subtypes. By incorporating diagnostic information to clustering and profiling the variability of both groups, the study provided a promising proof of concept in identifying ASD subtypes which are both biologically and clinically meaningful.

Given this improvement, however, there are remaining issues in the ASD subtyping research. First, which neuroimaging features would capture the main biological variability of autism is unclear, especially for those in functional magnetic resonance imaging (fMRI). Indeed, while numerous features have been proposed to reveal FC patterns specific to ASD (Maximo et al., 2013; Martínez et al., 2020; Cardinale et al., 2013), our understanding of atypical organization of functional brain systems in this condition remains incomplete. Notably, however, an emerging literature has reported a utility of dimensionality reduction techniques to represent large-scale FC as a series of low-dimensional spatial axes, each visualizing smoothly changing connectome transition along the cortical mantle (Margulies et al., 2016). This so-called '*connectome gradient*' metric has been recognized to effectively summarize high-dimensional connectome variations, for instance, those related to sensory-transmodal differentiation, in humans and non-human primates. Moreover, several clinical studies adopting this method showed high sensitivity in revealing pathological effects across multiple developmental conditions such as autism (Hong et al., 2019) and schizophrenia (Dong et al., 2020; Wang et al., 2020), demonstrating a potential as a useful imaging biomarker (S.J. Hong et al., 2020). Another issue in the current subtyping research is a lack of reproducibility assessment. Most previous subtyping results have been rarely tested using independent datasets, remaining as a proof of concept without a clear demonstration of whether they are not the consequence of overfitting to the given dataset or to hyperparameters for the employed clustering algorithm (Hosseini et al., 2020).

Here, we sought to address these critical issues by implementing a neurosubtyping framework that incorporates the connectome gradient into the functional random forest (FRF) and evaluating its reproducibility based on the Replication dataset from the open-sharing ASD data repositories (*i.e.,* Autism Brain Imaging Data Exchange, ABIDE-I/-II (Di Martino et al., 2014, 2017)). We constructed whole-brain connectome gradients from resting-state fMRI (rs-fMRI) of each individual using principal component analysis, which has been previously suggested to show a high predictive power for various phenotypic variables (S.J. Hong et al., 2020). In clustering ASD individuals, the FRF enabled our subtyping to utilize the features that are particularly specific to the targeted condition (=ASD). While the meaning of "specific to ASD" may vary depending on the context, here we chose the one that allows for predicting an ASD diagnostic label, and fed these ASD-specific features into the FRF (Feczko et al., 2018). We hypothesized that *i)* with such a clustering model constructed by diagnosis-informed features, reproducible and clinically useful subtypes can be recovered from heterogeneous individuals with autism, and *ii)* depending on which brain areas are affected in the functional gradients, group-level profiles of symptom severity may also vary across the identified neurosubtypes.

2. Method

2.1. Participants

We analyzed the two sets of multicentric neuroimaging data: *i)* Discovery (ABIDE-I (Di Martino et al., 2014); 143 Autism spectrum disorder [ASD] and 144 typically developing [TD] individuals) and *ii)* Replication (the ABIDE-II (Di Martino et al., 2017); 60 ASD and 59 TD) datasets. The former included only the subjects with a moderate-to-small head motion (framewise displacement < 0.3 mm) (Hong et al., 2019). Only the sites with at least 10 subjects were considered: NYU Langone Medical Center (NYU, 35/51, ASD/TD); University of Utah, School of Medicine (USM, 49/37, ASD/TD); University of Pittsburg, School of Medicine (Pitt, 19/20, ASD/TD), resulting in 211 subjects (103 ASD and 108 TD) in total. The age was not different between the groups (mean ± SD [years]: 20.8 ± 8.1 *vs.* 19.2 ± 7.1 for ASD and TD, respectively, $t = 1.54$, $p = 0.12$). The replication dataset was a total of 86 subjects (44 ASD and 42 TD) across the following sites: Trinity centre for Health Sciences, Trinity College Dublin (TCD, 15/17, ASD/TD); NYU Langone Medical Center (NYU, 20/18 ASD/TD); Institut Pasteur/Robert Debré Hospital (IP, 9/7 ASD/TD). This dataset did not show age differences between the two groups (mean ± SD [years]: 12.7 ± 5.2 *vs.* 14.1 ± 5.6 for ASD and TD, respectively, $t = 1.20$, $p = 0.23$). Still, to rule out the potential remaining effect from age, we regressed out this variable from main metrics (*i.e.,* functional gradient) using a statistical linear model in both discovery and replication datasets. We included only male individuals in our study, given their preponderant rate of occurrence. The symptom severity of ASD was assessed with Autism Diagnostic Observation Schedule (ADOS) total calibration score which takes into account for different language and age levels across the individuals, as well as subscores (*i.e.,* communication, social interaction, repeated behaviors/interests) and Social Responsiveness Scale (SRS) score (Constantino and Gruber, 2005; J.N. Constantino, and Gruber 2014). Table 1 has clinicodemographic variables for both datasets.

Table 1
Clinicodemographic variables.

		ASD	TD	ASD *vs* TD t (p-value)[1]	
N	Discovery	103	108		
	Replication	44	42		
Age (SD)		20.8 (8.1)	19.2 (7.1)	1.31 (0.19)	
		12.7 (5.2)	14.1 (5.6)	1.16 (0.24)	
IQ (SD)		104.4 (15.7)	114.2 (12.3)	4.72 (<0.001)	
		103.8 (22.5)	116.8 (19.2)	3.1 (<0.01)	
FD (SD)		0.094 (0.057)	0.083 (0.050)	1.48 (0.14)	
		0.114 (0.066)	0.078 (0.040)	2.72 (<0.01)	
Site	PITT		19 (18.4%)	20 (18.5%)	–
	USM		49 (47.6%)	37 (34.3%)	–
	NYU		35 (34%)	51 (47.2%)	–
	TCD		15 (34.1%)	17 (40.5%)	–
	NYU		20 (45.5%)	18 (42.9%)	–
	IP		9 (20.5%)	7 (16.7%)	–

Abbreviation: ASD, Autism spectrum disorder; TD, typically developing control; DS, discovery; RP, replication; SD, Standard deviation; FD, Framewise displacement. [1]The p value from two-sample t-tests between autism spectrum disorder and typically developing control datasets is reported. The elements for discovery set are colored by white, whereas those for replication by gray.

2.2. MRI acquisition

All sites provided T1-weighted (T1w) MRI and rs-fMRI that were scanned using 3T Siemens (NYU, PITT, USM) or Philips (TCD, IP) scanners (see Supplementary Table S1 for details).

2.3. Data preprocessing

The ABIDE-I database provided preprocessed T1w and rs-fMRI data, which are openly shared through the Preprocessed Connectomes initiative (http://preprocessed-connectomes-project.org/) (Craddock et al., 2013). Briefly, T1w structural data were preprocessed using FreeSurfer. The preprocessing pipeline includes gradient nonuniformity correction, registration to the stereotaxic space, intensity normalization, skull stripping, and white matter segmentation. White and pial surfaces were generated through triangular surface tessellation, topology correction, inflation, and spherical registration to fsaverage. The rs-fMRI data were preprocessed using the configurable pipeline for the analysis of connectomes (Cameron et al., 2013). The pipeline includes slice timing and head motion correction, skull stripping, and intensity normalization. White matter and cerebrospinal fluid signals were removed using the CompCor tool based on the top five principal components (Behzadi et al., 2007). Band-pass filtering (0.01 – 0.1 Hz) was applied, and the data were co-registered to MNI152 space. Surface alignment was confirmed for each individual, and voxel-wise rs-fMRI time-series were interpolated along the mid-thickness surface. While the original surface model was the Freesurfer fsaverage (160k vertices), to reduce the computational load as well as to take advantage of vertex-wise hemispheric symmetricity, the data were resampled to the Conte69 10k model of the Human Connectome Project (Van Essen et al., 2012; Glasser et al., 2016). Finally, the mapped fMRI timeseries were smoothed with a 5 mm full width at half maximum kernel. The same pipeline implemented in our group was applied to the ABIDE-II dataset for the image processing.

2.4. Subtyping using connectome gradient

Fig. 1 provides an overview of the proposed functional random forest (FRF) approach based on the connectome gradients.

2.4.1. Connectome gradient generation

We estimated the functional connectivity (FC) gradients from individual rs-fMRI data (Margulies et al., 2016). The cortex-wide FC matrix was constructed by Pearson's correlation of time series between every pair of the two brain areas, for which boundaries were defined by a multimodal parcellation atlas of Human Connectome Project (https://balsa.wustl.edu/) (Glasser et al., 2016). The resulting individual 360×360 FC matrices were harmonized for the site effects using Combat, a Bayesian approach to linearly regress out site effects by modeling site-specific scaling factors (Fortin et al., 2018). The correlation coefficients underwent Fisher's r-to-z transformation and were thresholded, leaving only the top 50% elements per row to remove relatively weaker connections spanning across the brain areas (see Results for the validation of this thresholding procedure). We derived functional gradients using principal component analysis (PCA), via Brainspace (https://github.com/MICA-MNI/BrainSpace) (Vos de Wael et al., 2020), as this has been demonstrated as having generally a high reliability and prediction power in our recent biomarker study (S.J. Hong et al., 2020). Group-level gradients were estimated in an unbiased manner using the averaged FC matrix from both ASD and TD cohorts, to which individual gradients were aligned based on the Procrustes algorithm (Langs et al., 2015). Apart from age, we also regressed out the effect of head motion (*i.e.,* FD) from the gradients based on a linear model, as in prior work (Hong et al., 2019).

Functional Random Forests. Before the main analyses, we first split the discovery dataset into training (60%) and validation (40%) samples for unbiased tests. The first gradient (=principal component score) of whole-brain connectivity from the training data was selected as an input for the FRF algorithm (see Results for the validation of component selection). Notably, prior to the FRF, we have performed feature selection to determine the candidate brain regions that can discriminate between the ASD and TD labels based on their gradient. To this end, we applied the least absolute shrinkage and selection operator (Tibshirani, 1996) to the whole-brain gradient values (of training samples), with the diagnostic labels as the response variable. This procedure served to reduce the feature search space for the random forest algorithm. The training of random forest was then conducted based on these selected features (see Supplementary Table S2). Briefly, randomly subsampling cases and features, the random forest iteratively built 1000 'weak' learners (*i.e.,* decision tree) to generate a final ensemble classifier which greatly improves both accuracy and generalizability of the classification. In this supervised learning process, the cases are naturally subgrouped in the leaf nodes, depending on their similarity of input data (=gradient values), which results in a proximity (or similarity) matrix. Each cell of this matrix indicates the number of times given two subjects were classified into the same label, thus becoming input for a following community detection algorithm (=Infomap, an unsupervised module of FRF) for the subtyping purpose (Rosvall and Bergstrom, 2008). It should be

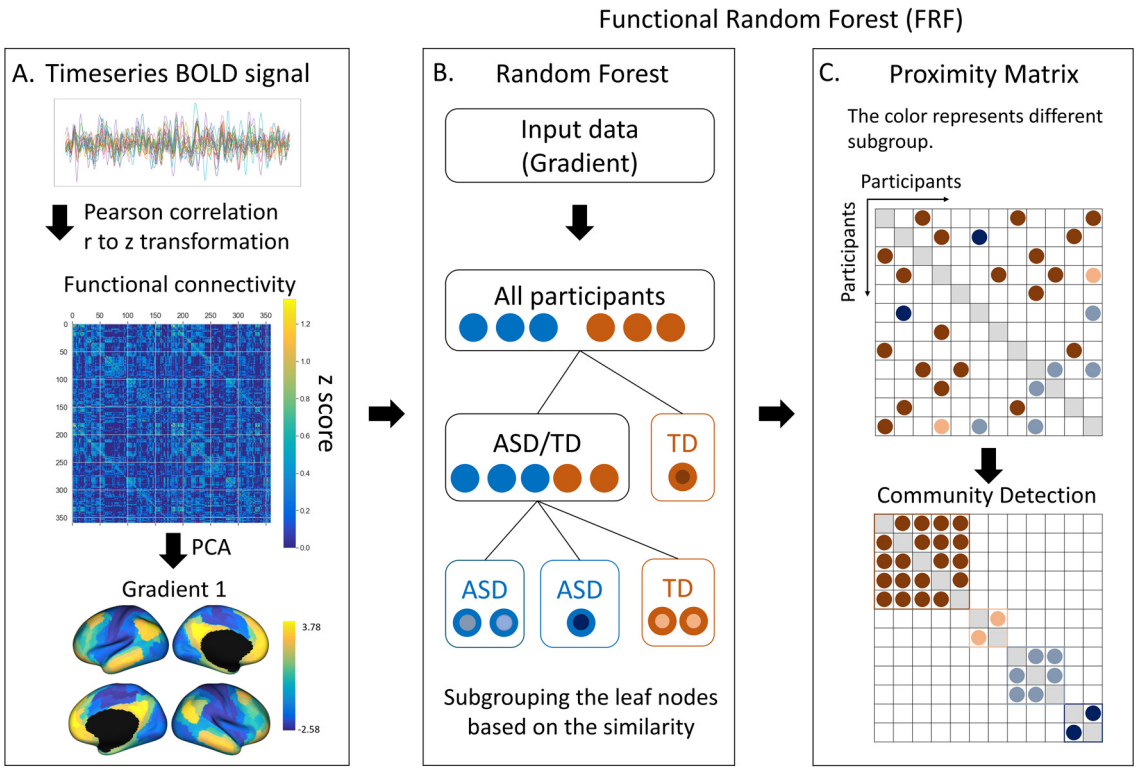

Fig. 1. Overview of the method. A. A FC matrix was constructed by Pearson correlation between the BOLD timeseries of the brain regions and *r-to-z* transformation. PCA was then applied to this FC matrix to yield connectome gradients. B-C. The gradient becomes an input to the following FRF algorithm, which was designed to classify each participant between the ASD and TD labels. This classification leads to generating a proximity matrix, where each cell represents the number of times that the two given participants fall into the same leaf node. The Infomap algorithm divides this proximity matrix into smaller subgroups, resulting in putative subtypes in the ASD and TD groups. *Abbreviations:* FC, functional connectivity; BOLD, blood oxygen level-dependent; PCA, principal component analysis; ASD, autism spectrum disorder; TD, typically developing control; FRF, functional random forest.

noted that this community detection was performed in both ASD and TD groups to compare the individual variabilities captured in ASD to those of the TD cohort. The algorithm used 1000 bootstraps to produce robust subtyping results.

2.5. Characterization of the ASD subtypes

The identified subtypes were profiled with respect to their whole-brain connectome gradients and symptom severity. For connectome gradients, we first assessed the differences between each ASD subtype and TD controls. We used a non-parametric rank-sum test on 360-ROIs whole-brain gradient values to compare the two groups (*e.g.,* ASD subtype *vs.* TD). The significant areas were then used as input to Neurosynth (Yarkoni et al., 2011; Rubin et al., 2017), a meta-analytical decoding database in order to evaluate which cognitive functions are generally associated to those brain areas. After this case-control comparison, the next analyses assessed the changes across the subtypes by performing a non-parametric one-way analysis of variance (ANOVA; Kruskal-Wallis H test) on the gradient values. Post-hoc analysis further compared the gradient values between each pair of ASD subtypes based on the rank-sum test. The use of non-parametric tests was to address unbalanced sample sizes across the identified subtypes (see Results). Following the brain profiling, we also assessed the behavioral relevance for the identified subtypes. Specifically, we compared the symptom severity scores measured by ADOS and SRS between the ASD subtypes using the rank-sum tests. The multiple comparisons across the brain regions and symptom severity scores were corrected using false-positive discovery rate (FDR) (Benjamini and Hochberg, 1995). To compute the effect size for the non-parametric rank-sum tests and Kruskal-Wallis H tests, effect size (r) and eta-squared measure (η^2) were computed (Tomczak and Tomczak, 2014).

2.6. Correlation between connectome gradient and degree centrality of FC

While the connectome gradient provides an effective summary for whole-brain functional organization, how the alteration in this feature is related to specific connectivity changes in local areas is often not clear. To further unpack connectivity alterations across identified subtypes, therefore, we targeted the brain areas showing significant gradient differences in ASD subtypes and correlated the differences in their gradient values with those of degree centrality (*i.e.,* a summed connectivity strength in a given brain area), which is one of the widely tested graph-theoretical measures for whole-brain network topology (Moseley et al., 2015; Tusche et al., 2014; Fallahi et al., 2021). Specifically, we computed the differences of gradients from all possible pairs of subjects in two subtypes (*e.g.,* if there are x and y subjects in the two subtypes respectively, in total $x \times y$ gradient difference values were aggregated from every pair of subjects). After performing the same aggregation for degree centrality as well, we correlated these two sets of difference values to contextualize the gradient changes from the connectivity perspective.

2.7. Reproducibility analysis

All analyses were repeated using a replication dataset. Notably, to test the generalizability of the subtypes, the exact FRF model trained using the training samples of discovery dataset was reused (*i.e.,* no further training), while only the input to this model was changed with the gradient values from the replication dataset, which resulted in its own (repli-

cation) proximity matrix. The Infomap identified the subtypes based on this proximity matrix. The profiles of subtypes (*i.e.,* gradient and ADOS scores) were then re-evaluated. Finally, we compared ADOS profiles across the subtypes between the discovery and replication datasets to quantitatively assess their generalizability.

2.8. Data and code availability

In performing these analyses, functional connectivity gradients were calculated based on the BrainSpace toolbox (https://brainspace.readthedocs.io/en/latest/), and the FRF was derived from (https://github.com/DCAN-Labs/functional-random-forest). All other codes that were used for main analyses (*e.g.*, statistical comparisons, control analysis, main running codes) in this study will be uploaded upon the acceptance of this paper (https://github.com/gudtls17/ASD.Neurosubtyping). The data analyzed in this study were all downloaded from ABIDE repositories: http://preprocessed-connectomes-project.org/ and http://fcon_1000.projects.nitrc.org/indi/abide/.

3. Result

3.1. Algorithmic validity of FRF

Before the main analyses, we first performed a simulation analysis to demonstrate if the FRF is indeed capable of properly subtyping the targeted features (*e.g.,* gradient) while tying the identified subtypes to the variables of interests (*e.g.,* diagnostic labels). For this, we created synthetic ASD and TD data (as analogous of gradient values) of the same sample size (=210) to the current study. We purposely made this data have three subtypes in each group by differentiating their global means, while adding the noise in the simulated features. As expected, the FRF could correctly identify 6 subtypes (3 for ASD and 3 for TD) with a moderate-to-high accuracy for diagnostic label classification across all datasets with different noises, which suggests the validity of FRF as a subtyping method. For full details of this control analysis, please see the Supplementary Material and Supplementary Figure S1.

3.2. Functional random forest

For the input to the FRF, we selected the first primary gradient (*i.e.,* 1st PC). This gradient was derived from the FC matrix which was top 50% row-wise thresholded in both ASD and TD groups. This particular analytical setting was chosen as it provided a maximum accuracy of the random forest algorithm (*i.e.,* diagnostic label prediction) in the validation samples of the discovery dataset, compared to that of other combinatory settings between the gradient order and threshold (see Supplementary Table S3 and Figures S2, S3). Indeed, when using the 1st gradient as an input for FRF, it correctly classified the label in the 73% in the training samples of discovery dataset, while yielding 58% of accuracy in the validation samples (Fig. 2), which results were significantly higher than a random chance and those from other component order of gradients ($p < 0.001$; permutation). Similar to the previous study (Margulies et al., 2016), our first gradient revealed the pattern of a cortical hierarchy stream differentiating the low-level sensory and high-order transmodal systems.

The subsequent application of the Infomap algorithm to the proximity matrix for the full discovery dataset revealed four putative subtypes in both ASD (n = 68, 14, 13, 8) and TD (n = 72, 20, 11, 5) groups (Fig. 2). To guarantee adequate statistical power in the following profiling analyses, we focused on those subtypes with ≥10 subjects, *i.e.,* ASD1 (n = 68), ASD2 (n = 14) and ASD3 (n = 13), and TD1 (n = 72), TD2 (n = 20) and TD3 (n = 11). For transparency, however, we also provided symptom severity profiles of those small samples of subtypes (n<10) (Supplementary Figure S4).

Directly applying this FRF model (trained by training samples of the discovery dataset) using the replication dataset led to a comparable classification accuracy of 60% (sensitivity: 50%, specificity: 69%), which was, again, significantly higher ($p < 0.001$) compared to the random chance (Fig. 2). While the accuracy seems only moderate, it in fact falls within the comparable range of previous studies (59–67%; Supplementary Table S4) (Heinsfeld et al., 2018; Niu et al., 2020; Plitt et al., 2015; Tejwani et al., 2017; Fredo et al., 2018), some of which have been conducted based on the rigorous setting of generalizability assessments (*e.g.,* leave-one-site out test). The subsequent community detection found 3 ASD subtypes (n = 18, 16, 10) similarly to the discovery findings, as well as 2 TD subtypes (n = 31, 11). As a baseline model, we also evaluated the subtyping results derived from the Infomap applied to the whole-brain functional gradient (*i.e.,* without the random forest classification). This analysis revealed only one subtype, suggesting no existence of statistically meaningful subgroups in the data (Supplementary Figure S5). This result highlights the necessity of tying the clustering algorithm to the main clinical variables in subtyping procedure.

Notably, the degree of head motion was not different between the discovery and replication datasets ($t = 0.87$, $p = 0.39$). While these subtypes found in both discovery and replication datasets did not show any noticeable association with head motion (ANOVA $F_{2,3}$<1.1, p>0.35), the site composition was found to be differential across the subtypes (ANOVA $F_{3,3}$,<10.52, $p = 0.03$; non-significant after FDR correction) (see the Supplementary Tables S5, S6). Although this may indicate a potential batch effect on the extraction of the subtypes, the facts that this is the result even after the successful ComBat (Supplementary Figure S6) process and that it did not occur in the replication nor in the typically developing brains (that are from the same data repositories) rule out the possibility of 100% attribution only to the batch effect but may reflect the true subtype profile as the data represents.

Notably, our analytical choice also included many other options related to a type of dimensionality reduction algorithms (to generate connectivity gradients), a statistical correction strategy for nuisance variables, with-*vs.*-without a feature selection procedure, and whether using multiple or single gradients. To demonstrate if our original setting was indeed the optimal one that provided us the best classification rate and subtyping results in a fully unbiased manner, we repeated all analyses above, systematically changing the analytical conditions. It should be noted that these analyses were all conducted based on the validation samples of the discovery data (without touching the replication data to avoid data leakage). First, when we tested Diffusion Embedding, a conventional non-linear dimensionality reduction algorithm, we obtained a lower accuracy for ASD-TD classification (accuracy=55%, sensitivity=50%, and specificity=60%; Supplementary Figure S7). Second, when we statistically corrected for site, age, and mean FD effects in a single linear model (instead of the Combat for the site effect followed by a separate statistical linear model for other nuisance variables, which is what we have done in this study), we observed a slightly worse classification rate (accuracy=54%, sensitivity=60%, and specificity=48%) and idiosyncratic subtyping results (*i.e.,* too many isolated small subgroups; Supplementary Figure S8). Third, when training the random forest without feature selection, the result was similarly suboptimal (accuracy = 48%, sensitivity = 51%, specificity = 45%, and identified subtypes included too small groups; Supplementary Figure S9). Finally, when merging multiple gradients, again we found a lower accuracy (accuracy = 50%, sensitivity = 59%, specificity = 42%) in the diagnostic label prediction. In sum, this series of control experiments confirmed the validity of our original analytical design.

3.3. Characteristics of ASD subtypes

Connectome gradient and cognitive profiles. After identifying the subtypes, we turned into in-depth profiling of their gradients. To this end, we first compared the functional gradient maps between ASD subtypes and TD groups but also directly between the ASD subtypes, assessing their specific brain anomalies.

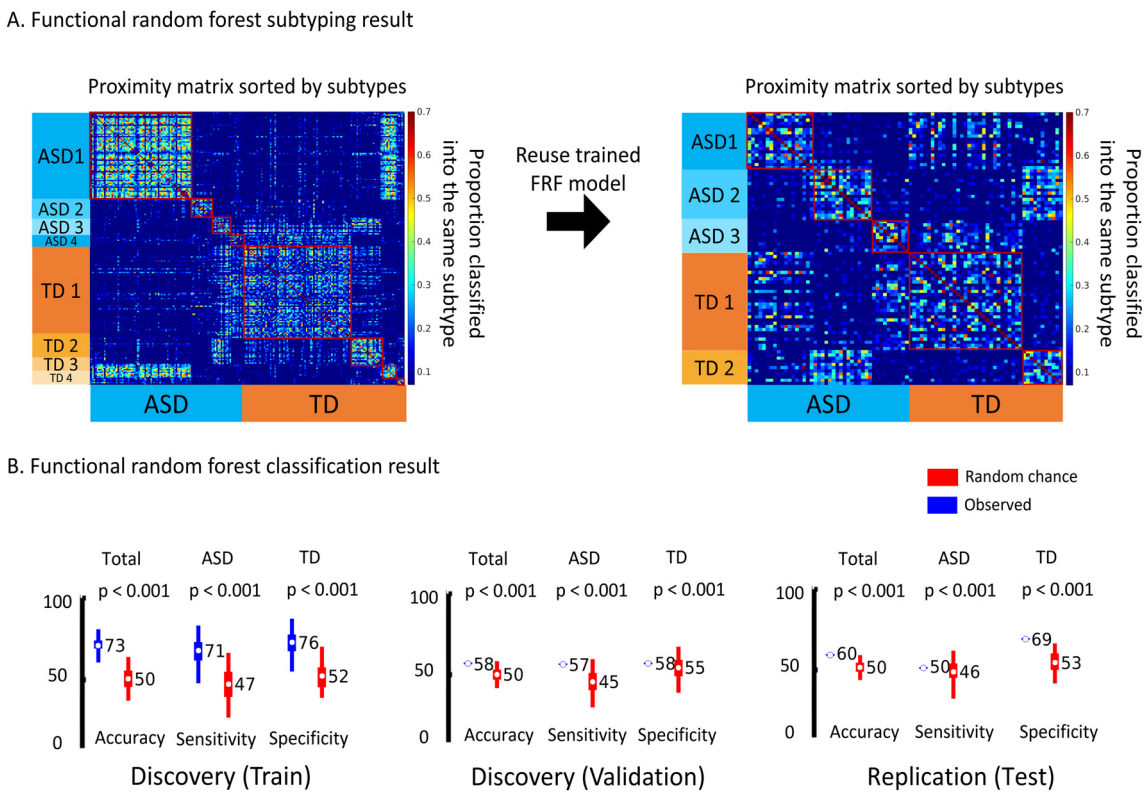

Fig. 2. The FRF results in discovery and replication datasets. The proximity matrix with the subgroups identified using Infomap (upper) as well as the classification accuracy of FRF (bottom) are presented (left: discovery, right: replication). For the proximity matrix, each row and column represent the participants, while the cell of the matrices indicates the number of times that the two given participants were classified into the same class using FRF models. *Abbreviations:* ASD, autism spectrum disorder; TD, typically developing control.

In the case-control comparison, multiple ASD-specific brain areas were observed across the subtypes. Specifically, ASD1 showed significant differences in the frontal, default mode, limbic, sensory-motor networks as well as the fusiform area (FDR=0.05, Fig. 3A, Supplementary Table S7). Subsequent Neurosynth-based analyses related these brain areas to multiple cognitive terms such as 'Default', 'Objects', 'Motor', and 'Somatosensory', which are relevant to major behavioral characteristics of autism (Assaf et al., 2010; Abbott et al., 2016; Cerliani et al., 2015). In ASD2, significant gradient differences were observed in the frontal, motor, and fusiform areas (FDR=0.05, Fig. 3B, Supplementary Table S8), which were also associated with the Neurosynth terms 'Congruent', 'Categories', 'Orthographic, and 'Visual word'. ASD3 showed no significant difference across the whole brain but only the tendency in the fusiform area (FDR=0.06, Fig. 3C, Supplementary Table S9). Brain regions involved in each subtype in the replication dataset were presented in the Supplementary Figure S10.

The ANOVA by which we compared the connectome gradients across the ASD subtypes revealed multiple brain areas showing a significant main group effect (Fig. 4A). When directly comparing between the ASD subtypes, differences were found in the frontal, sensory-motor, and default mode networks as well as fusiform areas between ASD1 and 2, the sensory-motor and auditory regions between subtype ASD1 and 3, and auditory regions and fusiform areas between ASD2 and 3 (Fig. 4B-D). In the post-hoc analysis, we found significant associations between the connectome gradients and graph-theoretical degree centrality metrics (FDR<0.001), which reflects underlying connectivity-level substrates for gradient changes across the subtypes.

Finally, the comparison within the TD groups (*i.e.,* TD1 *vs.* TD2 *vs.* TD3) revealed significant gradient differences in the brain areas that are both overlapped and distinct to those of ASD subtypes (Supplementary Figure S11). Indeed, similarity to the ANOVA result between the ASD subtypes (Fig. 4A), the inferior visual cortices as well as the precuneus areas were found to be different between TD subtypes, while the frontal areas (which showed significant gradient changes in ASD1) did not show any TD subtype-specific patterns. These results suggest that the gradient changes in each ASD subtype may be a mixture of both common and ASD-specific functional variations compared to the typically developed brain, suggesting a wide spectrum of ASD-related heterogeneity.

3.4. Symptom severity of the ASD subtypes

Distinct symptom profiles were found across the identified ASD subtypes (Table 2). Notably, depending on how much the gradient values were affected compared to TD, the symptom severity in ADOS (total calibration score) also systematically varied across the subtypes (*i.e.,* ASD1>ASD2>ASD3). Specifically, the ASD1 (showing the largest gradient changes) revealed marked tendency of differences in ADOS Total CSS (FDR=0.07) and communication (FDR=0.03) scores compared to ASD3 (Fig. 5A). In replication dataset, the ASD 1 revealed marked differences in ADOS Total CSS (FDR=0.04) and social (FDR=0.02) scores compared to ASD3. While the ASD2 also presented some differences in the ADOS social (FDR=0.04) scores compared to ASD 3 and the tendency in the Total CSS (FDR=0.05) and the communication (FDR=0.09) score compared to ASD 3, symptoms were overall milder compared to ASD1 (Fig. 5B). Most importantly, the subtypes derived from the discovery and replication datasets revealed highly similar symptom severity profiles (Fig. 5C), as supported by no statistical difference between the two datasets (Table 2, Supplementary Table S10). Taken together, our findings suggest that the identified subtypes have distinct symptom profiles, which were reproducible in the independent data.

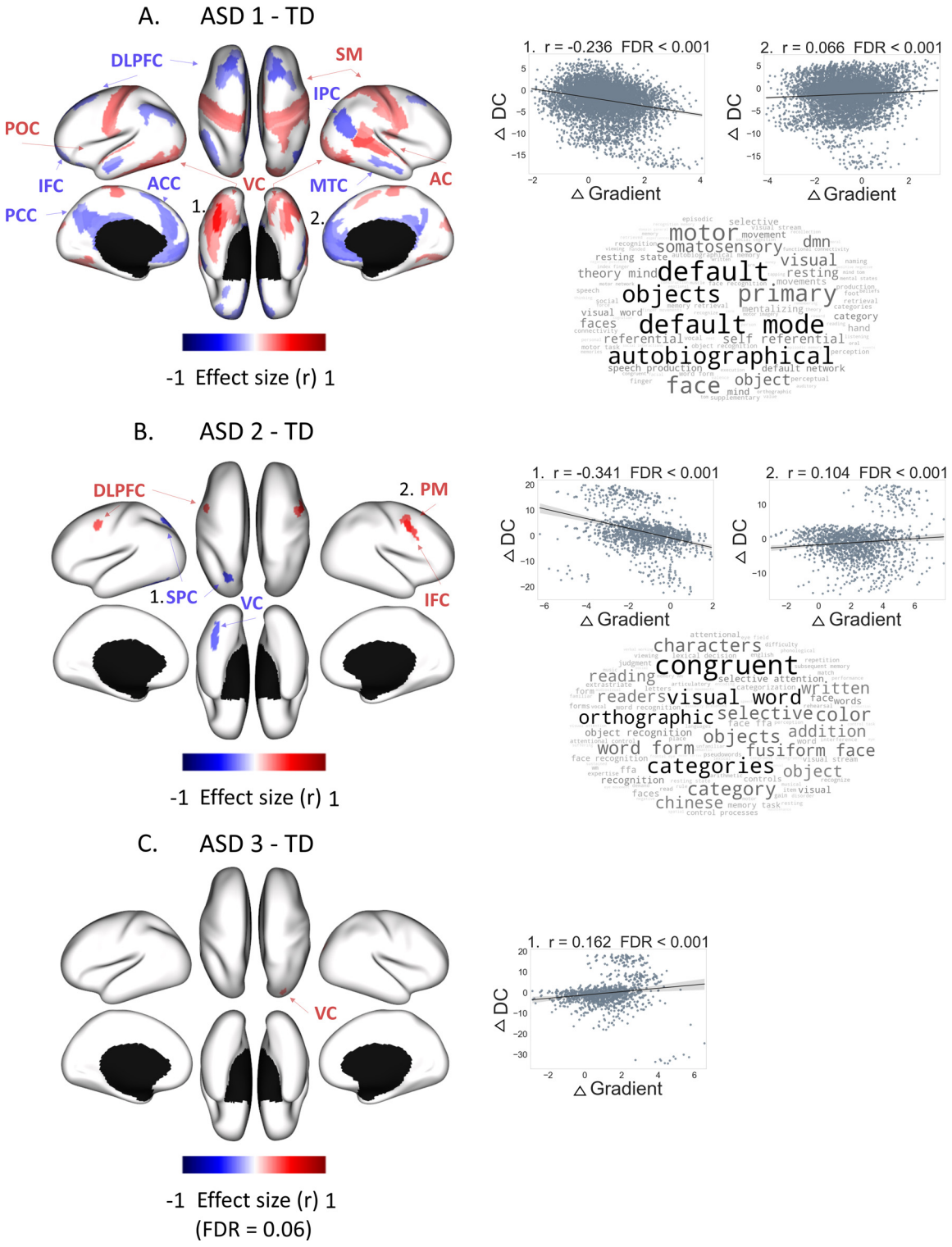

Fig. 3. Gradient differences between ASD subtypes and the TD group (discovery result). A. The brain areas showing a significant group difference in connectome gradients between ASD1 subtype and TD are presented with non-parametric effect size (*r*) (Tomczak and Tomczak, 2014). Among the significant areas, the parcels showing maximum statistics for increased and decreased gradients were chosen, and the differences of their gradient values and those of degree centrality were correlated to assess the connectivity-level change underlying the gradient differences (right scatter plots). Those significant areas were further decoded in terms of frequently associated cognitive functions using Neurosynth, which results were shown as a word cloud representation (under the scatter plots; bigger characters, higher a Neurosynth-correlation is). B-C. Results of the same analyses for ASD2 and ASD3 subtypes. *Abbreviations:* SM, somatosensory and motor cortex; PM, premotor cortex; DLPFC, dorsolateral prefrontal cortex; SPC, superior parietal cortex; IPC, inferior parietal cortex; IFC, inferior frontal cortex; MTC, medial temporal cortex; AC, early auditory cortex; VC, ventral stream visual cortex; ACC, anterior cingulate cortex; PCC, posterior cingulate cortex; POC, posterior opercular cortex.

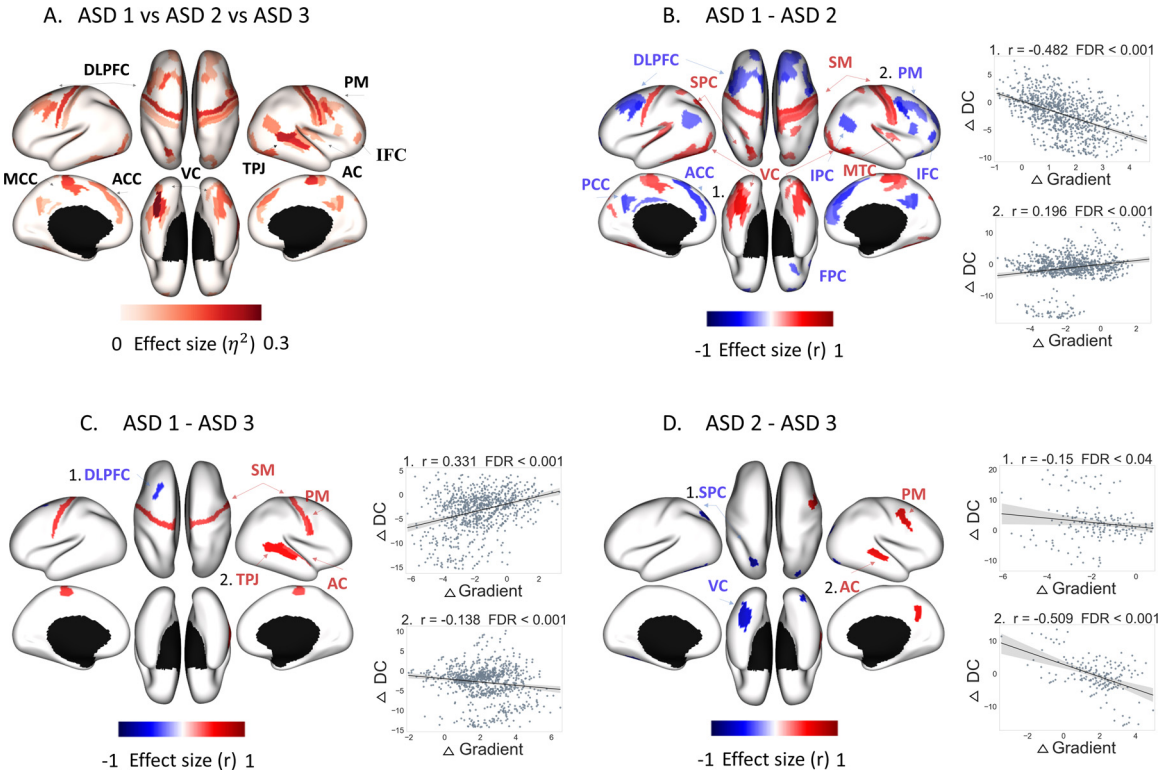

Fig. 4. Gradient differences between ASD subtypes (discovery result). A. The ANOVA result between three identified ASD subtypes is shown. The color indicates the eta-squared index (η^2) for the effect size of between-subtype differences. All significances are based on the FDR correction. B-D. The difference between each pair of subtypes is presented using non-parametric effect size (*r*). In the bottom of each panel, the scatter plots show the correlation between the differences in gradients and those in degree centrality of FC in the areas showing the largest group differences. *Abbreviations:* ANOVA, analysis of variance; SM, somatosensory and motor cortex; PM, premotor cortex; DLPFC, dorsolateral prefrontal cortex; SPC, superior parietal cortex; IPC, inferior parietal cortex; IFC, inferior frontal cortex; TPJ, temporal-parietal junction; MTC, medial temporal cortex; AC, early auditory cortex; VC, ventral stream visual cortex; ACC, anterior cingulate cortex; MCC, medial cingulate cortex; PCC, posterior cingulate cortex; FPC, fronto-polar cortex.

Table 2
Symptom severity across the subtypes between discovery (DS) and replication (RP) datasets.

	ASD1		p-value[1]	ASD2		p-value[1]	ASD3		p-value[1]
	DS	RP		DS	RP		DS	RP	
N	68	18		14	16		13	10	
ADOS Total CSS (SD)	7.02 (2.05)	6.28 (2.49)	0.20	6.93 (1.86)	6.31 (2.25)	0.44	6.08 (1.38)	4.40 (2.12)	0.04
ADOS comm (SD)	4.43 (1.52)	4.12 (1.71)	0.48	4.00 (1.24)	3.29 (1.82)	0.24	3.42 (1.44)	2.38 (0.74)	0.08
ADOS social (SD)	8.36 (2.80)	8.00 (2.83)	0.63	8.21 (2.61)	7.88 (2.66)	0.73	7.17 (1.95)	5.38 (1.41)	0.04
ADOS behavior (SD)	2.31 (1.46)	2.31 (1.84)	0.99	2.75 (1.04)	2.00 (0.58)	0.11	2.09 (1.04)	1.50 (0.71)	0.47
SRS (SD)	91.33 (31.59)	–		101.17 (36.22)	–		99.42 (37.00)	–	

Abbreviation: ADOS, autism diagnostic observation schedule; ADOS Total CSS, total calibration score; ADOS behavior, restricted and repetitive behavior; SRS, social responsiveness scale. DS, discovery; RP, replication; SD, Standard deviation.
[1] The p value from two sample t-tests between discovery and replication datasets is reported.

4. Discussion

Clinical heterogeneity remains a critical obstacle in the development of reliable diagnostic criteria in autism (Insel et al., 2010). While much effort has been recently made to build various subtyping strategies, those purely neuroimaging-based approaches may lack a component which can directly tie a main clinical question with an employed clustering algorithm. To address this issue, here we implemented a novel neurosubtyping framework combining whole-brain connectome gradient and the FRF clustering algorithm (Margulies et al., 2016; Feczko et al., 2018), which collectively allows discovering ASD subgroups showing reproducible symptom severity. We identified three dominant neurosubtypes in ASD and two subtypes in TD groups. These subtypes in ASD revealed distinct patterns of functional gradient anomalies in the areas that have been previously implicated in autism research (Uddin et al., 2013), such as default mode networks, sensory (*e.g.,* visual/auditory), and fusiform areas. Notably, they displayed an association between the extent of significant gradient changes (ASD1>2>3) and symptom severity across the subtypes. Indeed, ASD1 and 2 (showing relatively more abnormal gradients) showed the highest ADOS scores in Total CSS, social interaction and communication domains, while ASD3 (showing minimal gradient changes) presented only mild symptom severity across most of

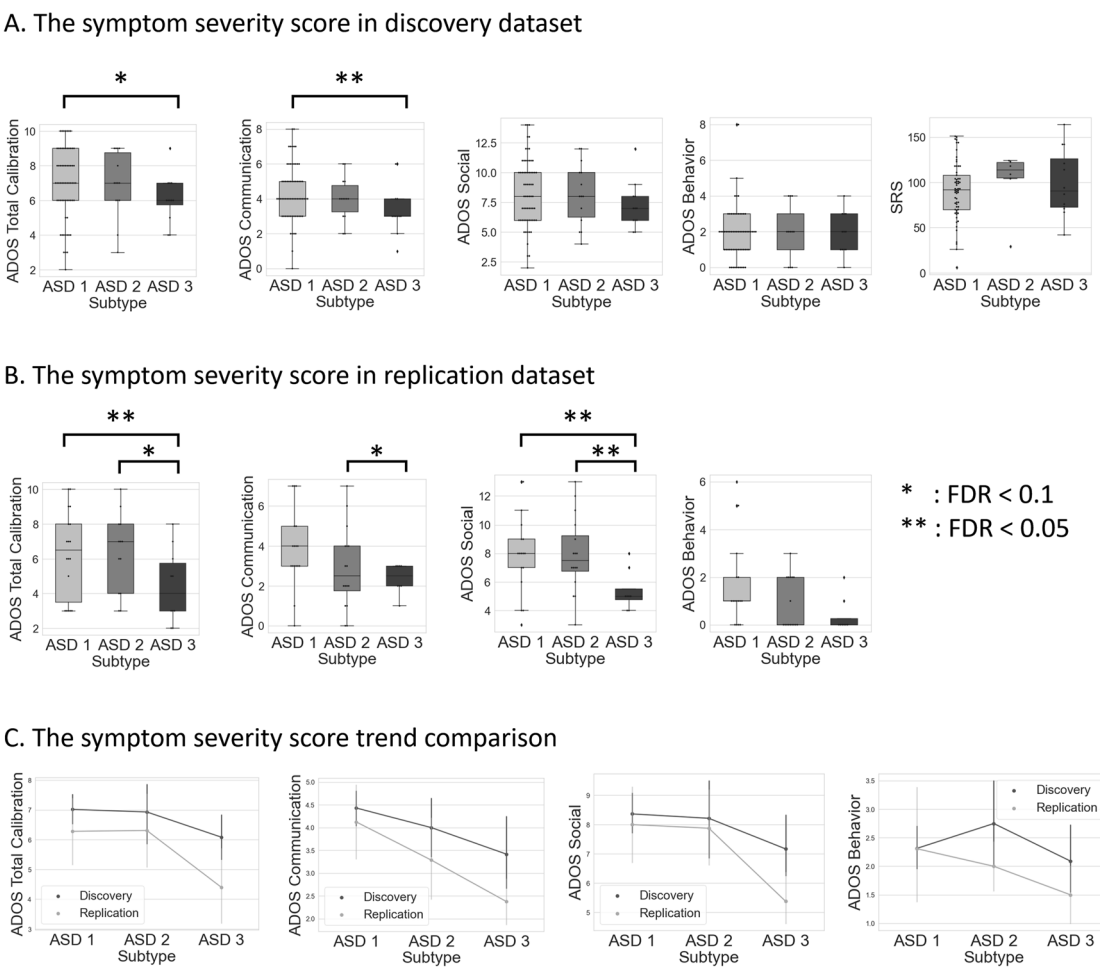

Fig. 5. The ADOS and SRS scores of each ASD subtype. A. For the discovery data, the distribution of symptom severity at each subtype is plotted across the domains (ADOS Total CSS, communication, social, repeated behaviors and SRS in order). B. The same plot for the replication data. C. The trends of symptom severity scores between the discovery and replication datasets are shown. SRS was excluded since it was not available for the replication set. The multiple comparisons were corrected using false positive discovery rate. Abbreviations: ASD, autism spectrum disorder; ADOS, autism diagnostic observation schedule; ADOS Total CSS, total calibration score; ADOS behavior, ADOS restricted and repetitive behavior; SRS, social responsiveness scale; FDR, false discovery rate.

the scores, suggesting a close relationship between their brains and behaviors. This subtype-dependent finding in symptom severity was preserved when analyzing the calibrated scores, which takes into account different age and language levels (Gotham et al., 2009). Most importantly, these phenotypic profiles across the subtypes were largely reproduced in the independent data (Fig. 5B and C), supporting high generalizability of our subtyping findings. Finally, when performing similar Infomap-based clustering on the whole-brain gradient without the random forest (*i.e.,* no involvement of a supervised classification), we did not find meaningful subgroups of ASD individuals, demonstrating a unique strength of the FRF approach.

In the current work, we opted to use functional gradients, recently proposed metrics to compress high-dimensional data of whole-brain connectivity, as input to neurosubtyping. We particularly selected the first principal component which functional connectome axis has been recently associated with autism as a potential pathogenic mechanism at the system level (Hong et al., 2019; Park et al., 2021). Specifically, this axis representing a large-scale cortical hierarchy stream showed less differentiation of functional connectivity (FC) in both low-level sensory and high-order transmodal systems in ASD, providing a parsimonious account to explain their altered sensory sensitivity and social impairment (Margulies et al., 2016). The current study relying on this gradient feature indeed found atypical connectivity profiles along this hierarchical axis (*i.e.,* a substantial decrease in the default mode network and increase in the sensory and fusiform areas) in ASD1, which subtype showed most deficits in social interaction and communication. Although of lower significance, ASD2 also showed contrasting effects between visual processing areas such as the fusiform and those situated in dorsal attention networks. Notably, ASD3 did not reveal any significant change in gradients compared to the TD group, mirroring the mild behavioral impairment in this ASD group. These findings collectively suggest that the functional network of ASD is characterized by deficits in more overarching principles of connectivity organizations (rather than in focal regions), and that the degree of this anomaly significantly varies across the individuals, which makes it challenging to detect it as a group-common signature of ASD at the actual clinical setting.

Apart from the selection of the first principal component as the main feature in this study, our algorithmic design leveraged a combination of several other methodological options, such as a dimensionality reduction algorithm (*i.e.*, PCA) and connectivity threshold (leaving only top 50%). Of note, this particular combination was based on the prediction accuracy in the validation samples from the training dataset. Thus, while

our particular choices in options were fully unbiased and data-driven, the selection of each option may also be explained by its unique advantage in studying the high-dimensional connectivity data. For instance, the use of PCA has been demonstrated to provide highly reliable functional gradient metrics as well as excellent prediction accuracy for various cognitive task performances (S.J. Hong et al., 2020). Regarding the connectivity threshold, normally a more stringent value (*e.g.*, 90–97%) provides a stronger case-control group (Dong et al., 2020) or aging effect (Bethlehem et al., 2020) in the neuroimaging studies, given its effect to remove noisy signals. Yet, in autistic individuals who are substantially heterogeneous, those peripheral connections (from a relatively lower threshold such as top 50%) in addition to the major backbone connectivity may sometimes have a more diagnostic power to separate an individual with ASD from neurotypicals. Indeed, in the recent study demonstrating a small number but highly generalizable subgroup of functional connectivity in classifying ASD (Yahata et al., 2016), those predictive ones generally have only a weak-to-moderate strength of connections, similar to what has been analyzed in our study. These previous findings collectively support the heuristic optimality of our algorithmic design, especially for subtyping high-dimensional and heterogeneous functional connectivity data.

As the ASD neurosubtyping studies, especially in the functional domain, are not fully mature, it is not straightforward to assess what specific commonalities and discrepancies exist between our and previous studies. Nevertheless, some convergence seems emerging at the global scale. First, as in most ASD functional neurosubtyping studies (Hong et al., 2018; Feczko et al., 2019; Wolfers et al., 2019), the identified subtypes in our study also revealed a combination of increases and decreases in functional gradients, which may be suggestive of both underlying mosaic manifestation of various etiologies and complementary effects during brain development related to the cortical plasticity. Second, for all neurosubtyping studies including ours have rarely been characterized by a spatially isolated pattern, but more distributed network systems in terms of brain anomalies. As our previous review (S.J. Hong et al., 2020) demonstrated relatively higher incidences of pathological effects in the transmodal systems across the subtypes, ASD 1 in our study also showed decreased functional gradient in the default mode areas, suggesting a potential vulnerability of these hub regions. Moreover, as recent studies increasingly revealed (Tang et al., 2020), the sensorimotor networks also seem to be affected in the functional brains of ASD, providing a potential system-level mechanism underlying their altered sensory sensitivity. While our subtype also showed similarly affected gradients in the same network, the absence of sensory-related phenotypic scores in the ABIDE dataset made it infeasible to precisely assess the behavior-brain relationship. One of the major differences between our and previous findings is that our subtypes also include those individuals with only mildly affected functional systems, which patterns are highly similar to neurotypical controls. It may be a signature of biological diversity in the autistic brains among which the extreme cases fall into even the normal developmental spectrum.

Our neurosubtyping model demonstrated reproducibility in the two different aspects. First, the FRF model trained by the discovery dataset (ABIDE I) showed a similar performance of ASD-*vs*-TD classification between the internal (discovery=58%) and external (ABIDE II replication=60%) validations. These results are also comparable to those of recent machine learning studies, confirming that our classification accuracy is not specific to the current dataset analyzed. In fact, while previous studies for ASD classification reported up to 90% of the accuracy in the initial period (Wolfers et al., 2019; Zhou et al., 2014), as the time passed and the sample size of the studies increased (possibly due to more availability of open-sharing data), the classification rate has constantly reduced to ~60%, suggesting a high likelihood of overfitting in the earlier work that normally had only small ASD cases. Indeed, one of the largest multi-site classification studies on ASD to date (using the ABIDE sample) performed a strict leave-one-site-out validation and reported ~60% inter-site prediction accuracy, which is not significantly beyond our result. Second, because of this optimized framework, we could demonstrate similar subtype-dependent symptom profiles between the discovery and replication datasets. Although showing a less degree of similarity compared to symptom severity, the functional gradient per se also showed similar brain areas of gradient difference between the discovery and replication datasets. Given that developing imaging markers to identify meaningful brain-symptom mapping is most prioritized in clinical neuroscience, future studies need to update their algorithms for better encoding of information from both brain and behaviors during the subtyping, such as recently demonstrated approaches, *e.g.,* Similarity Network Fusion (Wang et al., 2014) or Joint Individual Variance Explained (Yu et al., 2017).

A few points should be discussed to provide contextualized interpretation of our findings. First, our neurosubtyping validation was only based on ADOS/SRS symptom severity indices. As there are a multitude of other pathological and behavioral features that can characterize autism, our validation can be ideally more enriched by other strategies, including a longitudinal follow-up of behavioral intervention response or developmental brain changes across the subtypes. Second, our study focused on only neocortical FC as a target of neurosubtyping, yet there is a line of neuroimaging evidence indicating the role of subcortical and cerebellar cortices as important pathogenic models in autism (Stoodley et al., 2017; Limperopoulos et al., 2007). Future studies in ASD should therefore include these structures or even specifically target them as the main candidate for neurosubtyping. Third, our finding that both symptom severity and brain-level anomalies reveal monotonically increasing patterns between ASD subtypes may be the sign indicating that those changing patterns reflect normal neurodevelopmental stages, thus potentially a void effect of our subtyping framework for the treatment strategies. On the one hand, given evidence of shared genetics and biology between ASD and the general population (Bralten et al., 2018), this interpretation of our findings may not be merely fictitious, and thus reinforces the necessity to include normal samples in the autism neurosubtying study to better delineate the ASD-related heterogeneity. This evidence collectively suggests a highly spectral nature of autism diversity ranging from mildly to severely affected ASD anomalies, which have to be considered in future studies to develop new behavioral and genetic therapies for this heterogeneous condition.

The functional connectivity profiles of ASD individuals were previously reported to be differential according to the developmental age (Holiga et al., 2019; Henry et al., 2018). In this context, the slight performance gap between discovery and replication samples in our study may be due to the fact that these two datasets have different age ranges. This demographic difference resulted from the fact that the former dataset was screened to have both children and adult samples at the initial inclusion procedure, whereas the latter did not have such an explicit constraint during the process, which aimed to increase the sample spectrum in the generalizability test of our framework.

Finally, as much as we highlighted the importance of assessing typically developing brains to obtain a broader picture of ASD heterogeneity, comparing their brain variability to those of other developmental disorders is also a critical task. Inclusion of other conditions, such as attention-deficit hyperactivity disorder, schizophrenia or obsessive-compulsive disorder, might thus reveal shared and distinct underpinnings of heterogeneity in brain structure and function across neurodevelopmental disorders, a critical milestone to develop disease-tailored biomarkers for clinical diagnosis (Kernbach et al., 2018; Mitelman, 2019).

While many practical and biological issues remain to be resolved to understand the heterogeneity of ASD, the current neurosubtyping research is rapidly growing, owing to increasingly advanced statistical and pattern learning algorithms (Varoquaux, 2014). Paralleling these efforts, our diagnosis-informed and gradient-based neurosubtyping is also considered as a promising candidate for the integrated and clinically sensitive imaging biomarker framework, which will help the development of more objective stratification in ASD.

Data and code availability

In performing these analyses, functional connectivity gradients were calculated based on the BrainSpace toolbox (https://brainspace.readthedocs.io/en/latest/), and the FRF was derived from (https://github.com/DCAN-Labs/functional-random-forest). All other codes that were used for main analyses (*e.g.*, statistical comparisons, control analysis, main running codes) in this study will be uploaded upon the acceptance of this paper (https://github.com/gudtls17/ASD.Neurosubtyping). The data analyzed in this study were all downloaded from ABIDE repositories: http://preprocessed-connectomes-project.org/ and http://fcon_1000.projects.nitrc.org/indi/abide/.

Acknowledgment

This research was supported by National Research Foundation (NRF-2020M3E5D2A01084892, NRF-2021R1F1A1052303), Institute for Basic Science (IBS-R015-D1), Ministry of Science and ICT (IITP-2020-2018-0-01798), IITP grant funded by the AI Graduate School Support Program (2019-0-00421), ICT Creative Consilience program (IITP-2020-0-01821), Artificial Intelligence Convergence Research Center (IITP-2020-0-01389), and Artificial Intelligence Innovation Hub program (2021-0-02068). The work was also supported by funding from the Brain & Behavior Research Foundation (NARSAD Young Investigator grant; #28436). SLV was supported by Max Planck Gesellschaft (Otto Hahn award). MPM is supported by the Center for the Developing Brain at the Child Mind Institute, as well as NIMH R01MH081218, R01MH083246, and R21MH084126. BCB acknowledges research support from the National Science and Engineering Research Council of Canada (NSERC Discovery-1304413), Canadian Institutes of Health Research (CIHR FDN-154298, PJT-174995), SickKids Foundation (NI17-039), Azrieli Center for Autism Research (ACAR-TACC), Brain Canada, FRQ-S, and the Tier-2 Canada Research Chairs program. AM acknowledges research funding from NIEHS (R01 ES030950, R01 ES027424, 528 K23ES026239), NIH (1UG3OD023290), and the NVLD Project.

Supplementary materials

Supplementary material associated with this article can be found, in the online version, at doi:10.1016/j.neuroimage.2022.119212.

References

GUZE, S.B., 1995. Diagnostic and statistical manual of mental disorders, 4th ed. (DSM-IV). Am. J. Psychiatry. doi:10.1176/ajp.152.8.1228.

Ronald, A., Happé, F., Bolton, P., Butcher, L.M., Price, T.S., Wheelwright, S., Baron-Cohen, S., Plomin, R., 2006. Genetic heterogeneity between the three components of the autism spectrum: a twin study. J. Am. Acad. Child Adolesc. Psychiatry. doi:10.1097/01.chi.0000215325.13058.9d.

Masi, A., DeMayo, M.M., Glozier, N., Guastella, A.J., 2017. An overview of autism spectrum disorder, heterogeneity and treatment options. Neurosci. Bull. doi:10.1007/s12264-017-0100-y.

Kozak, M.J., Cuthbert, B.N., 2016. The NIMH research domain criteria initiative: background, issues, and pragmatics. Psychophysiology doi:10.1111/psyp.12518.

Hong, S.J., Valk, S.L., Di Martino, A., Milham, M.P., Bernhardt, B.C., 2018. Multidimensional neuroanatomical subtyping of autism spectrum disorder. Cereb. Cortex. doi:10.1093/cercor/bhx229.

Hong, S.J., Vogelstein, J.T., Gozzi, A., Bernhardt, B.C., Yeo, B.T.T., Milham, M.P., Di Martino, A., 2020a. Toward neurosubtypes in autism. Biol. Psychiatry doi:10.1016/j.biopsych.2020.03.022.

Feczko, E., Miranda-Dominguez, O., Marr, M., Graham, A.M., Nigg, J.T., Fair, D.A., 2019. The heterogeneity problem: approaches to identify psychiatric subtypes. Trends Cogn. Sci. doi:10.1016/j.tics.2019.03.009.

Wolfers, T., Floris, D.L., Dinga, R., van Rooij, D., Isakoglou, C., Kia, S.M., Zabihi, M., Llera, A., Chowdanayaka, R., Kumar, V.J., Peng, H., Laidi, C., Batalle, D., Dimitrova, R., Charman, T., Loth, E., Lai, M.C., Jones, E., Baumeister, S., Moessnang, C., Banaschewski, T., Ecker, C., Dumas, G., O'Muircheartaigh, J., Murphy, D., Buitelaar, J.K., Marquand, A.F., Beckmann, C.F., 2019. From pattern classification to stratification: towards conceptualizing the heterogeneity of Autism Spectrum Disorder. Neurosci. Biobehav. Rev. doi:10.1016/j.neubiorev.2019.07.010.

Chen, H., Uddin, L.Q., Guo, X., Wang, J., Wang, R., Wang, X., Duan, X., Chen, H., 2019. Parsing brain structural heterogeneity in males with autism spectrum disorder reveals distinct clinical subtypes. Hum. Brain Mapp. doi:10.1002/hbm.24400.

Easson, A.K., Fatima, Z., McIntosh, A.R., 2019. Functional connectivity-based subtypes of individuals with and without autism spectrum disorder. Netw. Neurosci. doi:10.1162/netn_a_00067.

Tang, S., Sun, N., Floris, D.L., Zhang, X., Di Martino, A., Yeo, B.T.T., 2020. Reconciling dimensional and categorical models of autism heterogeneity: a brain connectomics and behavioral study. Biol. Psychiatry. doi:10.1016/j.biopsych.2019.11.009.

Kanai, R., Rees, G., 2011. The structural basis of inter-individual differences in human behaviour and cognition. Nat. Rev. Neurosci. doi:10.1038/nrn3000.

Kernbach, J.M., Satterthwaite, T.D., Bassett, D.S., Smallwood, J., Margulies, D., Krall, S., Shaw, P., Varoquaux, G., Thirion, B., Konrad, K., Bzdok, D., 2018. Shared endophenotypes of default mode dsfunction in attention deficit/hyperactivity disorder and autism spectrum disorder. Transl. Psychiatry. doi:10.1038/s41398-018-0179-6.

Breiman, L., 2001. Random forests. Mach. Learn. doi:10.1023/A:1010933404324.

Rosvall, M., Bergstrom, C.T., 2008. Maps of random walks on complex networks reveal community structure. Proc. Natl. Acad. Sci. U. S. A. doi:10.1073/pnas.0706851105.

Maximo, J.O., Keown, C.L., Nair, A., Müller, R.A., 2013. Approaches to local connectivity in autism using resting state functional connectivity MRI. Front. Hum. Neurosci. doi:10.3389/fnhum.2013.00605.

Martínez, K., Martínez-García, M., Marcos-Vidal, L., Janssen, J., Castellanos, F.X., Pretus, C., Villarroya, Ó., Pina-Camacho, L., Díaz-Caneja, C.M., Parellada, M., Arango, C., Desco, M., Sepulcre, J., Carmona, S., 2020. Sensory-to-cognitive systems integration is associated with clinical severity in autism spectrum disorder. J. Am. Acad. Child Adolesc. Psychiatry. doi:10.1016/j.jaac.2019.05.033.

Cardinale, R.C., Shih, P., Fishman, I., Ford, L.M., Müller, R.A., 2013. Pervasive rightward asymmetry shifts of functional networks in autism spectrum disorder. JAMA Psychiatry doi:10.1001/jamapsychiatry.2013.382.

Margulies, D.S., Ghosh, S.S., Goulas, A., Falkiewicz, M., Huntenburg, J.M., Langs, G., Bezgin, G., Eickhoff, S.B., Castellanos, F.X., Petrides, M., Jefferies, E., Smallwood, J., 2016. Situating the default-mode network along a principal gradient of macroscale cortical organization. Proc. Natl. Acad. Sci. U. S. A. doi:10.1073/pnas.1608282113.

Hong, S.J., de Wael, R.V., Bethlehem, R.A.I., Lariviere, S., Paquola, C., Valk, S.L., Milham, M.P., Di Martino, A., Margulies, D.S., Smallwood, J., Bernhardt, B.C., 2019. Atypical functional connectome hierarchy in autism. Nat. Commun. doi:10.1038/s41467-019-08944-1.

Dong, D., Luo, C., Guell, X., Wang, Y., He, H., Duan, M., Eickhoff, S.B., Yao, D., 2020. Compression of cerebellar functional gradients in schizophrenia. Schizophr. Bull. doi:10.1093/schbul/sbaa016.

Wang, M., Li, A., Liu, Y., Yan, H., Sun, Y., Song, M., Chen, J., Chen, Y., Wang, H., Guo, H., Wan, P., Lv, L., Yang, Y., Li, P., Lu, L., Yan, J., Wang, H., Zhang, H., Zhang, D., Jiang, T., Liu, B., 2020. Reproducible abnormalities of functional gradient reliably predict clinical and cognitive symptoms in schizophrenia. BioRxiv doi:10.1101/2020.11.24.395251.

Hong, S.J., Xu, T., Nikolaidis, A., Smallwood, J., Margulies, D.S., Bernhardt, B., Vogelstein, J., Milham, M.P., 2020b. Toward a connectivity gradient-based framework for reproducible biomarker discovery. Neuroimage doi:10.1016/j.neuroimage.2020.117322.

Hosseini, M., Powell, M., Collins, J., Callahan-Flintoft, C., Jones, W., Bowman, H., Wyble, B., 2020. I tried a bunch of things: the dangers of unexpected overfitting in classification of brain data. Neurosci. Biobehav. Rev. doi:10.1016/j.neubiorev.2020.09.036.

Di Martino, A., Yan, C.G., Li, Q., Denio, E., Castellanos, F.X., Alaerts, K., Anderson, J.S., Assaf, M., Bookheimer, S.Y., Dapretto, M., Deen, B., Delmonte, S., Dinstein, I., Ertl-Wagner, B., Fair, D.A., Gallagher, L., Kennedy, D.P., Keown, C.L., Keysers, C., Lainhart, J.E., Lord, C., Luna, B., Menon, V., Minshew, N.J., Monk, C.S., Mueller, S., Müller, R.A., Nebel, M.B., Nigg, J.T., O'Hearn, K., Pelphrey, K.A., Peltier, S.J., Rudie, J.D., Sunaert, S., Thioux, M., Tyszka, J.M., Uddin, L.Q., Verhoeven, J.S., Wenderoth, N., Wiggins, J.L., Mostofsky, S.H., Milham, M.P., 2014. The autism brain imaging data exchange: towards a large-scale evaluation of the intrinsic brain architecture in autism. Mol. Psychiatry. doi:10.1038/mp.2013.78.

Di Martino, A., O'Connor, D., Chen, B., Alaerts, K., Anderson, J.S., Assaf, M., Balsters, J.H., Baxter, L., Beggiato, A., Bernaerts, S., Blanken, L.M.E., Bookheimer, S.Y., Braden, B.B., Byrge, L., Castellanos, F.X., Dapretto, M., Delorme, R., Fair, D.A., Fishman, I., Fitzgerald, J., Gallagher, L., Keehn, R.J.J., Kennedy, D.P., Lainhart, J.E., Luna, B., Mostofsky, S.H., Müller, R.A., Nebel, M.B., Nigg, J.T., O'Hearn, K., Solomon, M., Toro, R., Vaidya, C.J., Wenderoth, N., White, T., Craddock, R.C., Lord, C., Leventhal, B., Milham, M.P., 2017. Enhancing studies of the connectome in autism using the autism brain imaging data exchange II. Sci. Data. doi:10.1038/sdata.2017.10.

Feczko, E., Balba, N.M., Miranda-Dominguez, O., Cordova, M., Karalunas, S.L., Irwin, L., Demeter, D.V., Hill, A.P., Langhorst, B.H., Grieser Painter, J., Van Santen, J., Fombonne, E.J., Nigg, J.T., Fair, D.A., 2018. Subtyping cognitive profiles in Autism Spectrum Disorder using a Functional Random Forest algorithm. Neuroimage doi:10.1016/j.neuroimage.2017.12.044.

J.N. Constantino, C.P. Gruber, The Social Responsiveness Scale (SRS), 2005.

J.N. Constantino, & Gruber, 2014. Social Responsiveness Scale-Second Edition (SRS-2). J. Psychoeduc. Assess. doi:10.1111/j.1571-9979.2008.00196.x.

Craddock, C., Benhajali, Y., Chu, C., Chouinard, F., Evans, A., Jakab, A., Khundrakpam, B.S., Lewis, J.D., Li, Q., Milham, M., Yan, C., Bellec, P., 2013. The Neuro Bureau Preprocessing Initiative: open sharing of preprocessed neuroimaging data and derivatives. Front. Neuroinform..

Cameron, C., Sharad, S., Brian, C., Ranjeet, K., Satrajit, G., Chaogan, Y., Qingyang, L., Daniel, L., Joshua, V., Randal, B., Stanley, C., Maarten, M., Clare, K., Adriana, D.M., Francisco, C., Michael, M., 2013. Towards automated analysis of connectomes: the

configurable pipeline for the analysis of connectomes (C-PAC). Front. Neuroinform doi:10.3389/conf.fninf.2013.09.00042.
Behzadi, Y., Restom, K., Liau, J., Liu, T.T., 2007. A component based noise correction method (CompCor) for BOLD and perfusion based fMRI. Neuroimage doi:10.1016/j.neuroimage.2007.04.042.
Van Essen, D.C., Glasser, M.F., Dierker, D.L., Harwell, J., Coalson, T., 2012. Parcellations and hemispheric asymmetries of human cerebral cortex analyzed on surface-based atlases. Cereb. Cortex. doi:10.1093/cercor/bhr291.
Glasser, M.F., Coalson, T.S., Robinson, E.C., Hacker, C.D., Harwell, J., Yacoub, E., Ugurbil, K., Andersson, J., Beckmann, C.F., Jenkinson, M., Smith, S.M., Van Essen, D.C., 2016. A multi-modal parcellation of human cerebral cortex. Nature doi:10.1038/nature18933.
Fortin, J.P., Cullen, N., Sheline, Y.I., Taylor, W.D., Aselcioglu, I., Cook, P.A., Adams, P., Cooper, C., Fava, M., McGrath, P.J., McInnis, M., Phillips, M.L., Trivedi, M.H., Weissman, M.M., Shinohara, R.T., 2018. Harmonization of cortical thickness measurements across scanners and sites. Neuroimage doi:10.1016/j.neuroimage.2017.11.024.
Vos de Wael, R., Benkarim, O., Paquola, C., Lariviere, S., Royer, J., Tavakol, S., Xu, T., Hong, S.J., Langs, G., Valk, S., Misic, B., Milham, M., Margulies, D., Smallwood, J., Bernhardt, B.C., 2020. BrainSpace: a toolbox for the analysis of macroscale gradients in neuroimaging and connectomics datasets. Commun. Biol. doi:10.1038/s42003-020-0794-7.
Langs, G., Golland, P., Ghosh, S.S., 2015. Predicting activation across individuals with resting-state functional connectivity based multi-atlas label fusion. Lecture Notes Computer Science (Including Subser. Lecture Notes Artif. Intell. Lecture Notes Bioinformatics) doi:10.1007/978-3-319-24571-3_38.
Tibshirani, R., 1996. Regression Shrinkage and Selection Via the Lasso. J. R. Stat. Soc. Ser. B. doi:10.1111/j.2517-6161.1996.tb02080.x.
Yarkoni, T., Poldrack, R.A., Nichols, T.E., Van Essen, D.C., Wager, T.D., 2011. Large-scale automated synthesis of human functional neuroimaging data. Nat. Methods. doi:10.1038/nmeth.1635.
Rubin, T.N., Koyejo, O., Gorgolewski, K.J., Jones, M.N., Poldrack, R.A., Yarkoni, T., 2017. Decoding brain activity using a large-scale probabilistic functional-anatomical atlas of human cognition. PLoS Comput. Biol. doi:10.1371/journal.pcbi.1005649.
Benjamini, Y., Hochberg, Y., 1995. Controlling the false discovery rate: a practical and powerful approach to multiple testing. J. R. Stat. Soc. Ser. B. doi:10.1111/j.2517-6161.1995.tb02031.x.
Tomczak, M., Tomczak, E., 2014. The need to report effect size estimates revisited. An overview of some recommended measures of effect size. Trends Sport Sci.
Moseley, R.L., Ypma, R.J.F., Holt, R.J., Floris, D., Chura, L.R., Spencer, M.D., Baron-Cohen, S., Suckling, J., Bullmore, E., Rubinov, M., 2015. Whole-brain functional hypoconnectivity as an endophenotype of autism in adolescents. NeuroImage Clin doi:10.1016/j.nicl.2015.07.015.
Tusche, A., Smallwood, J., Bernhardt, B.C., Singer, T., 2014. Classifying the wandering mind: revealing the affective content of thoughts during task-free rest periods. Neuroimage doi:10.1016/j.neuroimage.2014.03.076.
Fallahi, A., Pooyan, M., Lotfi, N., Baniasad, F., Tapak, L., Mohammadi-Mobarakeh, N., Hashemi-Fesharaki, S.S., Mehvari-Habibabadi, J., Ay, M.R., Nazem-Zadeh, M.R., 2021. Dynamic functional connectivity in temporal lobe epilepsy: a graph theoretical and machine learning approach. Neurol. Sci. doi:10.1007/s10072-020-04759-x.
Heinsfeld, A.S., Franco, A.R., Craddock, R.C., Buchweitz, A., Meneguzzi, F., 2018. Identification of autism spectrum disorder using deep learning and the ABIDE dataset. NeuroImage Clin doi:10.1016/j.nicl.2017.08.017.
Niu, K., Guo, J., Pan, Y., Gao, X., Peng, X., Li, N., Li, H., 2020. Multichannel deep attention neural networks for the classification of autism spectrum disorder using neuroimaging and personal characteristic data. Complexity doi:10.1155/2020/1357853.
Plitt, M., Barnes, K.A., Martin, A., 2015. Functional connectivity classification of autism identifies highly predictive brain features but falls short of biomarker standards. NeuroImage Clin doi:10.1016/j.nicl.2014.12.013.
R. Tejwani, A. Liska, H. You, J. Reinen, P. Das, Autism classification using brain functional connectivity dynamics and machine learning, ArXiv. (2017).
Fredo, A.R.J., Jahedi, A., Reiter, M., Muller, R.A., 2018. Diagnostic classification of autism using resting-state fMRI data and conditional random forest. Conf. Proc. ... Annu. Int. Conf. IEEE Eng. Med. Biol. Soc. IEEE Eng. Med. Biol. Soc. Annu. Conf. doi:10.1109/EMBC.2018.8512502.
Assaf, M., Jagannathan, K., Calhoun, V.D., Miller, L., Stevens, M.C., Sahl, R., O'Boyle, J.G., Schultz, R.T., Pearlson, G.D., 2010. Abnormal functional connectivity of default mode sub-networks in autism spectrum disorder patients. Neuroimage doi:10.1016/j.neuroimage.2010.05.067.
Abbott, A.E., Nair, A., Keown, C.L., Datko, M., Jahedi, A., Fishman, I., Müller, R.A., 2016. Patterns of atypical functional connectivity and behavioral links in autism differ between default, salience, and executive networks. Cereb. Cortex. doi:10.1093/cercor/bhv191.
Cerliani, L., Mennes, M., Thomas, R.M., Di Martino, A., Thioux, M., Keysers, C., 2015. Increased functional connectivity between subcortical and cortical resting-state networks in Autism spectrum disorder. JAMA Psychiatry doi:10.1001/jamapsychiatry.2015.0101.
Insel, T., Cuthbert, B., Garvey, M., Heinssen, R., Pine, D.S., Quinn, K., Sanislow, C., Wang, P., 2010. Research Domain Criteria (RDoC): toward a new classification framework for research on mental disorders. Am. J. Psychiatry. doi:10.1176/appi.ajp.2010.09091379.
Uddin, L.Q., Supekar, K., Menon, V., 2013. Reconceptualizing functional brain connectivity in autism from a developmental perspective. Front. Hum. Neurosci. doi:10.3389/fnhum.2013.00458.
Gotham, K., Pickles, A., Lord, C., 2009. Standardizing ADOS scores for a measure of severity in autism spectrum disorders. J. Autism Dev. Disord. doi:10.1007/s10803-008-0674-3.
Park, B., Hong, S.-J., Valk, S.L., Paquola, C., Benkarim, O., Bethlehem, R.A.I., Di Martino, A., Milham, M.P., Gozzi, A., Yeo, B.T.T., Smallwood, J., Bernhardt, B.C., 2021. Differences in subcortico-cortical interactions identified from connectome and microcircuit models in autism. Nat. Commun. doi:10.1038/s41467-021-21732-0.
Bethlehem, R.A.I., Paquola, C., Seidlitz, J., Ronan, L., Bernhardt, B., Consortium, C.C.A.N., Tsvetanov, K.A., 2020. Dispersion of functional gradients across the adult lifespan. Neuroimage doi:10.1016/j.neuroimage.2020.117299.
Yahata, N., Morimoto, J., Hashimoto, R., Lisi, G., Shibata, K., Kawakubo, Y., Kuwabara, H., Kuroda, M., Yamada, T., Megumi, F., Imamizu, H., Náñez, J.E., Takahashi, H., Okamoto, Y., Kasai, K., Kato, N., Sasaki, Y., Watanabe, T., Kawato, M., 2016. A small number of abnormal brain connections predicts adult autism spectrum disorder. Nat. Commun. doi:10.1038/ncomms11254.
Zhou, Y., Yu, F., Duong, T., 2014. Multiparametric MRI characterization and prediction in autism spectrum disorder using graph theory and machine learning. PLoS ONE doi:10.1371/journal.pone.0090405.
Wang, B., Mezlini, A.M., Demir, F., Fiume, M., Tu, Z., Brudno, M., Haibe-Kains, B., Goldenberg, A., 2014. Similarity network fusion for aggregating data types on a genomic scale. Nat. Methods. doi:10.1038/nmeth.2810.
Yu, Q., Risk, B.B., Zhang, K., Marron, J.S., 2017. JIVE integration of imaging and behavioral data. Neuroimage doi:10.1016/j.neuroimage.2017.02.072.
Stoodley, C.J., D'Mello, A.M., Ellegood, J., Jakkamsetti, V., Liu, P., Nebel, M.B., Gibson, J.M., Kelly, E., Meng, F., Cano, C.A., Pascual, J.M., Mostofsky, S.H., Lerch, J.P., Tsai, P.T., 2017. Altered cerebellar connectivity in autism and cerebellar-mediated rescue of autism-related behaviors in mice. Nat. Neurosci. doi:10.1038/s41593-017-0004-1.
Limperopoulos, C., Bassan, H., Gauvreau, K., Robertson, R.L., Sullivan, N.R., Benson, C.B., Avery, L., Stewart, J., Soul, J.S., Ringer, S.A., Volpe, J.J., Du Plessis, A.J., 2007. Does cerebellar injury in premature infants contribute to the high prevalence of long-term cognitive, learning, and behavioral disability in survivors? Pediatrics doi:10.1542/peds.2007-1041.
Bralten, J., Van Hulzen, K.J., Martens, M.B., Galesloot, T.E., Arias Vasquez, A., Kiemeney, L.A., Buitelaar, J.K., Muntjewerff, J.W., Franke, B., Poelmans, G., 2018. Autism spectrum disorders and autistic traits share genetics and biology. Mol. Psychiatry. doi:10.1038/mp.2017.98.
Holiga, Š., Hipp, J.F., Chatham, C.H., Garces, P., Spooren, W., D'Ardhuy, X.L., Bertolino, A., Bouquet, C., Buitelaar, J.K., Bours, C., Rausch, A., Oldehinkel, M., Bouvard, M., Amestoy, A., Caralp, M., Gueguen, S., Le Moal, M.L., Houenou, J., Beckmann, C.F., Loth, E., Murphy, D., Charman, T., Tillmann, J., Laidi, C., Delorme, R., Beggiato, A., Gaman, A., Scheid, I., Leboyer, M., d'Albis, M.A., Sevigny, J., Czech, C., Bolognani, F., Honey, G.D., Dukart, J., 2019. Patients with autism spectrum disorders display reproducible functional connectivity alterations. Sci. Transl. Med. doi:10.1126/scitranslmed.aat9223.
Henry, T.R., Dichter, G.S., Gates, K., 2018. Age and gender effects on intrinsic connectivity in autism using functional integration and segregation. Biol. Psychiatry Cogn. Neurosci. Neuroimaging. doi:10.1016/j.bpsc.2017.10.006.
Mitelman, S.A., 2019. Transdiagnostic neuroimaging in psychiatry: a review. Psychiatry Res doi:10.1016/j.psychres.2019.01.026.
Varoquaux, G., Thirion, B., 2014. How machine learning is shaping cognitive neuroimaging. Gigascience doi:10.1186/2047-217X-3-28.